

Control Parameter Extraction Model for Reconfigurable Bandpass Filter Based on Bayesian Optimized Multiple-Output XGBoost

Jian Shi^{ID}, Jiancheng Dong^{ID}, Zhenyu Wang^{ID}, *Graduate Student Member, IEEE*,
 Bin Liu^{ID}, *Graduate Student Member, IEEE*, Tao Yang^{ID}, Yong Wang^{ID},
 Sheng Wang^{ID}, and Jihong Shen

Abstract—This letter proposes a control parameter extraction (CPE) model for the reconfigurable bandpass filter (RBPF) to achieve fast reconfiguration of center frequency and bandwidth. The CPE model consists of an automatic hyperparameter generation (AHG) module and a multioutput XGBoost (MO-XGB) module. AHG, based on Bayesian optimization, is used to generate the MO-XGB module hyperparameters. Through experiments on the fabricated circuit, the model extracted the control parameters of RBPFs in 15 ms with root mean square error (RMSE) of 0.0098 and 0.0129 for center frequency and bandwidth, respectively. Therefore, the model's effectiveness has been proven.

Index Terms—Bayesian optimization, control parameter, reconfigurable bandpass filter (RBPF), XGBoost (XGB).

I. INTRODUCTION

ECONFIGURABLE bandpass filters (RBPFs) are receiving more and more attention due to their advantages in significantly reducing system size and complexity. Many studies [1], [2], [3] worked on designing RBPF's critical functions, including frequency and bandwidth reconfigurability.

In practical applications of RBPFs, such as electronic countermeasures scenarios, the control parameters of RBPFs need to be adjusted quickly to realize the fast switching of center frequency or bandwidth. Therefore, control parameter extraction (CPE) is the key to realize the fast and accurate reconfigurability of RBPFs. Both CPE and design parameter extraction (DPE) are the inverse modeling of the RBPFs. The difference is that CPE is a fast adjustment of the control

Manuscript received 3 December 2023; accepted 11 December 2023. Date of publication 15 January 2024; date of current version 13 March 2024. (Corresponding authors: Jian Shi; Jihong Shen.)

Jian Shi and Jihong Shen are with the College of Intelligent Systems Science and Engineering, Harbin Engineering University, Harbin 150001, China (e-mail: sj2019@hrbeu.edu.cn; shenjihong@hrbeu.edu.cn).

Jiancheng Dong is with the Research Center of Advanced RF Chips and Systems, Nanhu Laboratory, Jiaxing 314001, China.

Zhenyu Wang and Yong Wang are with the School of Information and Communication Engineering, University of Electronic Science and Technology of China, Chengdu 610054, China.

Bin Liu and Tao Yang are with the School of Electronic Science and Engineering, University of Electronic Science and Technology of China, Chengdu, Sichuan 610054, China.

Sheng Wang is with the Northern Institute of Electronic Equipment, Beijing 100191, China.

Color versions of one or more figures in this letter are available at <https://doi.org/10.1109/LMWT.2023.3343095>.

Digital Object Identifier 10.1109/LMWT.2023.3343095

parameters of the reconfigurable filter with known physical parameters and upper and lower bounds of the adjustable interval, usually in milliseconds, while DPE allows a certain amount of time to be consumed to optimize the design, which can be several hours or more. The inverse modeling of microwave devices can be divided into the optimization method and the direct inverse model method [4]. The optimization approach requires repeated forward model evaluations, whereas the direct inverse model approach immediately provides an inverse solution after completing the training. Consequently, the direct inverse model approach is quicker than the optimization approach [5].

Machine learning has been used for the direct inverse modeling of microwave devices, and in particular, neural networks are considered an efficient tool for microwave modeling and optimization [6], [7], [8], [9], [10]. In addition to neural networks, other machine-learning methods can be utilized for microwave modeling. XGBoost (XGB) [11] model works very well for classification or regression problems. However, the traditional XGB regression model has only one output and craves the labor-intensive selection of appropriate hyperparameters to obtain good performance.

This letter innovatively proposes a CPE model for RBPFs to achieve fast reconfiguration of center frequency and bandwidth. Within the model, a serial multiple-output XGB (MO-XGB) module is designed to construct a multioutput regressor, and a Bayesian optimization-based automatic hyperparameter generation (AHG) module is designed to improve the model's performance. The experimental results demonstrate that the CPE model outperforms the traditional multiple output regression model.

II. PROPOSED METHOD

A. CPE Model Architecture

The proposed CPE model is a multiple-input and multiple-output regression model, as shown in Fig. 1. The model's inputs are the RBPFs' electromagnetic response (e.g., center frequency, bandwidth, and insertion loss). In contrast, its outputs are the RBPFs' control parameters (e.g., capacitance values of variable capacitors). Moreover, the CPE model comprises an AHG module and an MO-XGB module. The AHG module contains an MO-XGB module hyperparameter generation method based on Bayesian optimization to generate

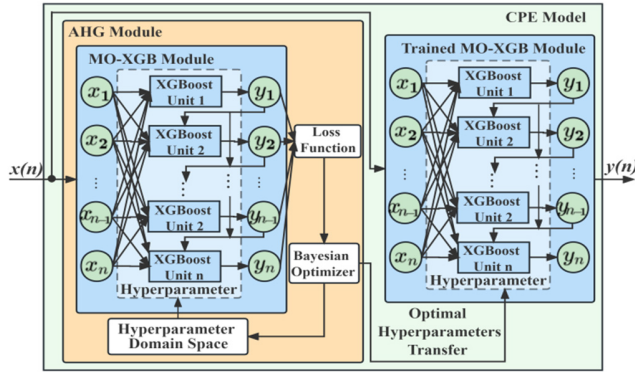


Fig. 1. Proposed CPE model.

the MO-XGB module accurately and quickly. The MO-XGB module fits one regressor to each output. The corresponding output can be obtained by examining the corresponding regressor, where each regressor submodule uses the XGB model.

B. MO-XGB Module

XGB is a modified machine-learning model stemming from the boosting algorithm and implements an additive model based on several classification and regression trees. Each new decision tree is added as the base learner to fit the residuals of the previous prediction. The final results of the prediction model are obtained by accumulating the prediction results of all decision trees [11].

The traditional XGB model has only one output. The m outputs model based on parallel structure MO-XGB (P-MO-XGB) module can be designed as

$$\hat{\mathbf{y}} = \{f_{\text{xgb_}1}(\mathbf{x}), f_{\text{xgb_}2}(\mathbf{x}), \dots, f_{\text{xgb_}i}(\mathbf{x})\}, \quad i = 1, 2, \dots, m \quad (1)$$

where \hat{y} is the predicted vector, and f_{xgb_i} means the i th parallel structure XGB submodule.

Considering the interaction relationship between the control parameters of the model output, a serial structure MO-XGB (S-MO-XGB) module is designed to connect the submodules. The serial structure uses the output of the previous submodule as the input of the next submodule. The i th output expression of S-MO-XGB model is formulated as

$$\hat{y}_i = \begin{cases} f_{\text{xgb}_i}(\mathbf{x}), & i = 1 \\ f_{\text{xgb}_i}(\mathbf{x}, \hat{y}_1, \dots, \hat{y}_{i-1}), & i > 1. \end{cases} \quad (2)$$

The output vector \hat{y} of S-MO-XGB model with m outputs is defined as

$$\hat{y} = \{\hat{y}_1, \hat{y}_2, \dots, \hat{y}_m\}$$

$$\hat{y}_i = \begin{cases} f_{xgb_i}(\mathbf{x}), & i = 1 \\ f_{xgb_i}(\mathbf{x}, \hat{y}_1, \dots, \hat{y}_{i-1}), & 1 < i \leq m. \end{cases} \quad (3)$$

We define \mathbf{h} to represent a vector containing all the hyperparameters of the entire MO-XGB model. The error function of MO-XGB model with m outputs $E(\mathbf{h})$ is designed as the mean square error corresponding to each output. The error function expression of n samples and m outputs is defined as

$$E(\mathbf{h}) = \frac{1}{n} \sum_{i=1}^n (y_i - \hat{y}_i)^2 = \frac{1}{n \times m} \sum_{i=1}^n \left(\sum_{j=1}^m (y_{ij} - \hat{y}_{ij})^2 \right) \quad (4)$$

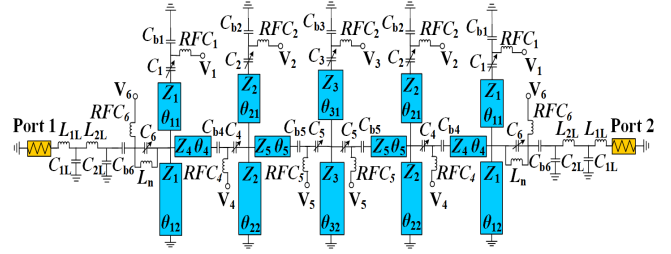


Fig. 2. Equivalent circuit model of the microstrip RBPF.

where \hat{y}_i is the i th predicted vector and y_i means the i th actual vector in n samples.

C. AHG Module

Hyperparameter optimization of the MO-XGB module can improve prediction accuracy and generalization. The Bayesian optimization method is applied for AHG module.

The fundamental principle of Bayesian optimization involves continually adding sample points to update the posterior objective function distribution under the circumstance of the given optimization objective function. For the hyperparametric optimization problem of the MO-XGB model, in a set of hyperparametric decision spaces, Bayesian optimization is used to construct a probabilistic model for the function $g : \mathbf{H} \rightarrow \mathbb{R}^n$ to be optimized. Furthermore, use the model to select the next evaluation point and then iterate the loop to obtain the hyperparameter optimal solution [12].

$$\mathbf{H}^* = \arg \max_{\mathbf{h} \in \mathcal{H}} g(\mathbf{h}) \quad (5)$$

where \mathbf{H}^* is the optimal hyperparameter combination, \mathbf{H} is the hyperparameter domain space, and $g(\mathbf{h})$ is the objective function.

The multioutput objective function $g(\mathbf{h})$ is designed as the inverse of the $E(\mathbf{h})$. According to (4), the objective function expression is defined as

$$g(\mathbf{h}) = (E(\mathbf{h}))^{-1} = \left(\frac{1}{n \times t} \sum_{i=1}^n \left(\sum_{j=1}^m (\hat{y}_{ij} - y_{ij})^2 \right) \right)^{-1}. \quad (6)$$

We maximize the value of the objective function $g(\mathbf{h})$ by Bayesian optimization to minimize the value of the loss function $E(\mathbf{h})$ to approach the hyperparameter optimal solution.

III. EXPERIMENTAL RESULTS

An RBPF is fabricated as an example of the CPE model. The equivalent circuit model in Agilent Technologies Advanced Design System (ADS) is shown in Fig. 2. The circuit is fabricated on a Rogers RO4330B substrate with a thickness of 0.508 mm. The RBPF is controlled by 11 silicon Schottky diodes, model SMV1248, from Skyworks. The dc bias circuit consists of the 100-pf capacitors and the 100k resistors [13], [14]. Because of the symmetry, the 11 diodes are controlled by six channels of voltage. The lower and upper bounds of the varactor are 0 and 8 V, respectively. The center frequency adjustment range is 0.8–1.4 GHz. The fabricated circuit photograph is shown in Fig. 3.

The experimental setup consists of a host computer program, a six-channel digital-to-analog voltage converter module, and an electronic network analyzer (ENA) network analyzer, as shown in Fig. 4. The aforementioned six channels

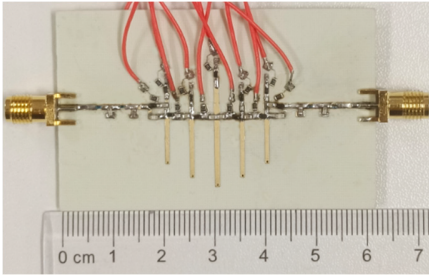


Fig. 3. Fabricated circuit photograph of the microstrip RBPF.

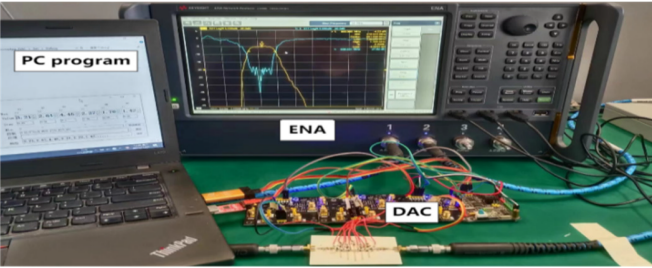


Fig. 4. Experimental setup.

TABLE I

DOMAIN SPACE AND OPTIMAL HYPERPARAMETERS

Hyperparameter	Domain space		P-MO-XGB	S-MO-XGB
	Low limit	Upper limit	Optimization	Optimization
learning_rate	0.01	0.2	0.0751	0.0662
max_depth	3	8	7	5
n_estimators	100	500	183	102
min_child_weight	0	10	1.5637	0.8561
subsample	0.1	1	0.7615	0.7031
colsample_bytree	0.1	1	0.3604	0.5356

of voltage are taken as an input for a series of parametric in fabricated circuit to obtain the magnitude of the scattering parameters S_{11} and S_{21} by the ENA network analyzer.

The input of the proposed CPE model is $\mathbf{x} = [f_c, \text{BW}]^T$, with f_c representing the center frequency and BW representing the bandwidth. The model's output is six channels of voltage $\mathbf{y} = [v_1, v_2, v_3, v_4, v_5, v_6]^T$.

The hyperparameter domain space of MO-XGB is created before Bayesian optimization, which describes the range of values to be evaluated and then find the optimal hyperparameters in the domain space. The domain space and the optimal hyperparameter combinations are shown in Table I. Those parameters not involved in the optimization use the algorithm's default values.

For comparison, the traditional multiple-output regression model and the proposed method are compared in PYTHON. Commonly used multiple output regression models include support vector regression (SVR) and multilayer perceptron (MLP). Among them, the MLP model is a three-layer MLP, and the optimal number of hidden neurons obtained after Bayesian optimization is 92.

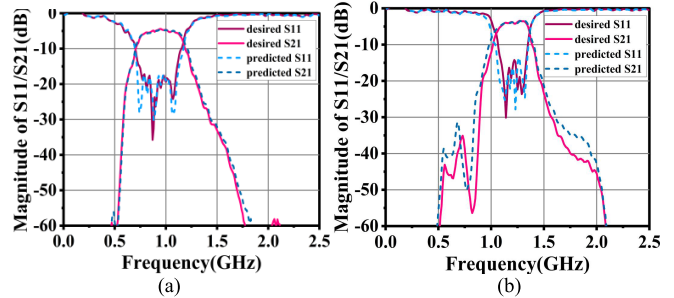
Table II shows the comparison between different models. The computational hardware is an Intel¹ Core² i7-7500 CPU at 2.90 GHz. The error function $E(\mathbf{h})$ was used to assess the model's accuracy according to (4), and mean absolute error (MAE) and root mean square error (RMSE) were also employed to evaluate the accuracy of predicted voltage

¹Registered trademark.²Trademarked.TABLE II
COMPARISON BETWEEN DIFFERENT MODELING METHODS

Methods	$E(\mathbf{h})$	MAE	RMSE	CPU time
SVR	0.2256	0.3488	0.4354	0.0025s
MLP	0.2467	0.3792	0.4706	0.0010s
P-MO-XGB	0.0853	0.2039	0.2614	0.0130s
S-MO-XGB	0.0767	0.1560	0.2137	0.0150s

TABLE III
COMPARISON OF THE DESIRED AND PREDICTED RESPONSE

Methods	f_c (GHz)		BW(GHz)	
	MAE	RMSE	MAE	RMSE
SVR	0.0425	0.0558	0.0390	0.0445
MLP	0.0238	0.0283	0.0306	0.0419
P-MO-XGB	0.0130	0.0147	0.0138	0.0184
S-MO-XGB	0.0062	0.0098	0.0113	0.0129

Fig. 5. Comparison of S -parameters between the desired and predicted control parameter. (a) CP1 and (b) CP2.

values. The proposed MO-XGB models significantly improve accuracy, and S-MO-XGB is better than P-MO-XGB. The proposed model is applied in the scenario of predicting RBPF control parameters, so the CPU time is considered only for a single regression prediction process and not the time required to train the model. The CPU time consumed by the proposed mode for each prediction operation is 15 ms.

The output values $\mathbf{y} = [v_1, v_2, v_3, v_4, v_5, v_6]^T$ predicted by the above method were configured into the fabricated circuits, and then, forward measurements were performed to obtain the S -parameters using an ENA network analyzer. The RBPF response (f_c , BW) is obtained by calculating the S -parameters. MAE and RMSE are employed to calculate the variance between the responses and the raw dataset, as shown in Table III. The MAE and RMSE of the S-MO-XGB model are smaller than that of the SVR, the MLP, and the P-MO-XGB, which indicates that the S-MO-XGB is the most accurate model among them. For visualization, we choose two sets of desired bandpass responses, as shown in Fig. 5. The test results show that once the MO-XGB module is built by the AHG module, the model will reliably and quickly predict the control parameters of RBPFs.

IV. CONCLUSION

This letter presents a CPE model for RBPF based on Bayesian optimization and MO-XGB, which has been verified in a fabricated circuit and enables accurate and fast dynamic configuration of multiple functions on the same RBPF hardware platform. The future direction may be to consider more filter responses as inputs and to correlate further between each output to increase the role of the correlation of each output on the model results.

REFERENCES

- [1] X. Zhu, T. Yang, P.-L. Chi, and R. Xu, "Novel reconfigurable single-to-balanced, power-dividing, and single-ended filter with frequency and bandwidth control," *IEEE Trans. Microw. Theory Techn.*, vol. 67, no. 2, pp. 670–682, Feb. 2019.
- [2] X. Zhu, T. Yang, P.-L. Chi, and R. Xu, "Novel reconfigurable filtering rat-race coupler, branch-line coupler, and multiorder bandpass filter with frequency, bandwidth, and power division ratio control," *IEEE Trans. Microw. Theory Techn.*, vol. 68, no. 4, pp. 1496–1509, Apr. 2020.
- [3] M. Fan, K. Song, and Y. Fan, "Reconfigurable bandpass filter with wide-range bandwidth and frequency control," *IEEE Trans. Circuits Syst. II, Exp. Briefs*, vol. 68, no. 6, pp. 1758–1762, Jun. 2021.
- [4] H. Kabir, Y. Wang, M. Yu, and Q.-J. Zhang, "Neural network inverse modeling and applications to microwave filter design," *IEEE Trans. Microw. Theory Techn.*, vol. 56, no. 4, pp. 867–879, Apr. 2008.
- [5] Z. Wang, F. Yan, S. Ma, T. Yang, H. Shao, and Y. Wang, "A synthesis-analysis machine with self-inspection mechanism for automatic design of on-chip inductors based on artificial neural networks," *IEEE Trans. Circuits Syst. I, Reg. Papers*, vol. 69, no. 10, pp. 4154–4167, Oct. 2022.
- [6] F. Feng, W. Na, J. Jin, J. Zhang, W. Zhang, and Q.-J. Zhang, "Artificial neural networks for microwave computer-aided design: The state of the art," *IEEE Trans. Microw. Theory Techn.*, vol. 70, no. 11, pp. 4597–4619, Nov. 2022.
- [7] F. Feng, W. Na, J. Jin, W. Zhang, and Q.-J. Zhang, "ANNs for fast parameterized EM modeling: The state of the art in machine learning for design automation of passive microwave structures," *IEEE Microw. Mag.*, vol. 22, no. 10, pp. 37–50, Oct. 2021.
- [8] J. Jin, C. Zhang, F. Feng, W. Na, J. Ma, and Q.-J. Zhang, "Deep neural network technique for high-dimensional microwave modeling and applications to parameter extraction of microwave filters," *IEEE Trans. Microw. Theory Techn.*, vol. 67, no. 10, pp. 4140–4155, Oct. 2019.
- [9] Y. Wu, G. Pan, D. Lu, and M. Yu, "Artificial neural network for dimensionality reduction and its application to microwave filters inverse modeling," *IEEE Trans. Microw. Theory Techn.*, vol. 70, no. 11, pp. 4683–4693, Nov. 2022, doi: [10.1109/TMTT.2022.3161928](https://doi.org/10.1109/TMTT.2022.3161928).
- [10] J. Cui, F. Feng, W. Na, and Q.-J. Zhang, "Bayesian-based automated model generation method for neural network modeling of microwave components," *IEEE Microw. Wireless Compon. Lett.*, vol. 31, no. 11, pp. 1179–1182, Nov. 2021.
- [11] T. Chen and C. Guestrin, "XGBoost: A scalable tree boosting system," in *Proc. 22nd ACM Sigkdd Int. Conf. Knowl. Discovery Data Mining*, 2016, pp. 94–785.
- [12] J. Snoek, H. Larochelle, and R. P. Adams, "Practical Bayesian optimization of machine learning algorithms," in *Proc. Adv. Neural Inf. Process. Syst.*, 2012, pp. 2951–2959.
- [13] H.-M. Lee and G. M. Rebeiz, "A 640–1030 MHz four-pole tunable filter with improved stopband rejection and controllable bandwidth and transmission zeros," in *IEEE MTT-S Int. Microw. Symp. Dig.*, Seattle, WA, USA, Jun. 2013, pp. 1–3, doi: [10.1109/MWSYM.2013.6697603](https://doi.org/10.1109/MWSYM.2013.6697603).
- [14] L. Gao and G. M. Rebeiz, "A 0.97–1.53-GHz tunable four-pole bandpass filter with four transmission zeroes," *IEEE Microw. Wireless Compon. Lett.*, vol. 29, no. 3, pp. 195–197, Mar. 2019, doi: [10.1109/LMWC.2019.2895558](https://doi.org/10.1109/LMWC.2019.2895558).